Dynamic impact of wheeled skidders on forest soil in felling areas

Igor Grigorev [a,*], Ol'ga Kunickaya [a], Evgeniy Tikhonov [b], Edward Hertz [c], Varvara Druzyanova [d], Oksana Timokhova [e], Viktor Ivanov [f], Igor Kruchinin [g]

[a] Department of Technology and Equipment of Forest Complex, Arctic State Agrotechnological University, Yakutsk, Russian Federation
[b] Department of Transport and Technological Machinery and Equipment, Petrozavodsk State University, Petrozavodsk, Russian Federation
[c] Department of Technologies and Equipment of Timber Industry, Ural State Forest Engineering University, Yekaterinburg, Russian Federation
[d] Department of Operation of Road Transport and Auto Repair, Northeastern Federal University Named After MK Ammosov, Yakutsk, Russian Federation
[e] Department of Engineering Technological Machines and Equipment, Ukhta State Technical University, Ukhta, Russian Federation
[f] Department of Forest Crops, Breeding and Dendrology, Bratsk State University, Bratsk, Russian Federation
[g] Department of Transport and Road Construction, Ural State Forestry University, Yekaterinburg, Russian Federation

ARTICLE INFO

ABSTRACT

Soil compaction from wheeled vehicles poses a huge challenge for the forest ecosystems. Modeling the impact of skidding machines on the soil could help solve the problem. The present work seeks to construct a mathematical model of soil compaction under the cyclic dynamic loading of wheeled skidding machines using the vibration analysis method for elastic dynamic systems. The study found that 4×4, 6×6 and 8×8 forestry vehicles have similar amplitude-frequency characteristics regardless of driving speed and load. The analysis of soil compaction from dynamic loading revealed that loaded and unloaded skidder passes cause the least damage (21–31%) to forest roads compared to skid trails. As regards skid trails, 4×4 and 6×6 tractors were found to compact the soil by 23–50% in the first four passes. The subsequent passes will lead to 60–66% of compaction. Finally, 8×8 trucks cause 98–99% of soil compaction. The difference between the experimental and theoretical values of soil density does not exceed 12%. The unevenness coefficient of the soil compaction and the confidence interval fall within the acceptable range. The mathematical models are in good agreement with the experimental data and can be used to calculate the operating modes of wheeled forestry equipment.

© 2022 ISTVS. Published by Elsevier Ltd. All rights reserved.

1. Introduction

The advancement of technology and high demand for forest products stimulate the logging activity with large-sized machinery and heavy equipment. The machines are wheeled and track-driven forwarders, skidders, harvesters, log trucks, etc. (Kremers and Boosten, 2018). Each causes damage to the forest soil, affecting its physical properties (Cambi et al., 2017; Ugawa et al., 2020). The primary impact of machinery is soil compaction – a factor crucial to ecosystem functions and soil biodiversity, and often leading to erosion and water imbalance (Cambi et al., 2018; Mohieddinne et al., 2019; Spinelli et al., 2019).

Soil compaction from large-sized machinery and heavy equipment is more severe than from lighter machines, altering the physical properties of the soil to a greater extent (Parkhurst et al., 2018; Tavankar et al., 2021a). The transportation of logs to the nearest terminal is carried out by skidders, the passing of which leads to

rut formation and displacement of soil (Parkhurst et al., 2018). The speed of soil compaction depends on soil type and structure, its moisture content, climatic conditions, steepness of slopes along the path, number of passes with forest equipment, and the type of tires used in wheeled skidders (Allman et al., 2020; Bigelow et al., 2018; Naghdi et al., 2017; Sealey and Van Rees, 2019). Many experimental studies on the effect of forestry equipment on the soil show that the most significant changes occur in the upper layer of the soil (Abukari et al., 2021; Aust et al., 2020; Parkhurst et al., 2018). In addition, the first two or three passes compact the soil more than subsequent passes (Vantellingen and Thomas, 2021). Moreover, moderate soil compaction can create less favorable conditions for the alteration of nutrient balance and microorganisms' activity (Solgi et al., 2019b). Therefore, the impact of forestry equipment on the soil is still open to debate; it is needful to develop a mathematical model to investigate the influence of various factors on soil compaction.

The negative impact of forest machines and skidding operations on the soil can be evaluated using a specific methodology, which means that the investigation should have a scientifically grounded

structure, be logically organized, and involve appropriate research methods (Tavankar et al., 2021b). Theoretical research usually involves the analysis of theoretical solutions. This study examines a range of mathematical models for predicting soil compaction under equipment loading (Ivanov et al., 2018; Manukovsky et al., 2018; Rudov et al., 2019; Solgi et al., 2019a; Yazarlou et al., 2017). According to the control theory, each control problem contains four elements (Lynch, 2020): (1) a controlled object or system; (2) a target output value; (3) a set of admissible controls; and (4) the effectiveness of control actions. In this case, the forest soil exposed to compaction stress during forestry operations can be considered a controlled system. Its future behavior is completely determined by the state of the system and future control action. The desired output value would be the minimal soil compaction upon completion of the skidding process. Because each skid trail has individual properties, it is necessary to determine the optimal skidding method, skidder model, and optimal speed of movement to ensure the maximum pass count possible before the acceptable soil compaction is achieved. The complexity of exploring the tractor/bundle-of-logs/soil system is that the solution elements do not lend themselves to ranking, and the number of possible solutions is low.

The widely used method to study skidder's impact at different weight and power ratios is simple enumeration optimization with the limited number of installed engine power options (Ahmad, 1989), which demonstrates good accuracy. Another method, amplitude-frequency characteristics (AFC), is used based on the results of the vehicle dynamics study (Grigorev et al., 2020b).

This work seeks to study the impact that different types of skidding equipment have on the soil by looking at their amplitude-frequency characteristics and to establish the optimal operating mode to minimize soil compaction. For this, the study uses a vibration model of the elastic dynamic system with the Laplace transform. It enables determining the amplitude-frequency characteristics of the skidding equipment. The objectives of the study are to determine the overall soil compaction from a wheeled skidder based on AFC calculations and assess whether or not mathematical models of soil compaction from a wheeled tractor are effective (reliability test).

2. Materials and methods

The vibrations of elastic dynamic systems are often used to study the operating conditions of multi-axle and sprung vehicles and agricultural machines (Grigorev et al., 2020a, 2020c, 2021). An example is a two-axle tractor of mass $т_T$, which carries logs of mass $т_L$. In this case, the mass $т_C$ of the whole system would be concentrated at the center of mass. The road profile is set as a random variable by the correlation function for the impact $R(\tau_i)$ taking into account the variations in height of the road surface D (0.7–1.3 cm^2) (Grigorev, 2005):

$$R(\tau_i) = De^{-\alpha|\tau_i|} \cos \beta\tau_i \qquad (1)$$

where: α and β are empirical coefficients, and τ_i is the time interval between the first wheel hitting the irregular surface and the i-th wheel hitting it, expressed as:

$$\tau_i = \frac{l_1 - l_i}{v} \qquad (2)$$

where: l_i denotes the spatial distance between the axles and the center of mass of the system moving with speed v.

Since the dynamic vibrations of a skidder is a holonomy system with constant parameters, the motion of such a system can be considered in an inertial coordinate system, where the equations of motion are provided for the principle of equilibrium of the acting forces using the principle of d'Alembert.

Here are the differential equations for the vertical (Z) and longitudinal-angular (φ) vibrations of a linear dynamic system:

$$\begin{cases} \ddot{Z} + a_1\dot{Z} + a_2 Z = \frac{1}{m_c}\left(\sum_{i=1}^{2n}\mu_t \dot{J}_i + \sum_{i=1}^{2n} C_t J_i\right) \\ \ddot{\varphi} + b_1\dot{\varphi} + b_2\varphi = \frac{1}{J_{lp}}\left(\sum_{i=1}^{2n}\mu_t l_i\dot{J}_i + \sum_{i=1}^{2n} C_t l_i J_i\right) \end{cases} \qquad (3)$$

$$a_1 = \frac{2n\mu_t}{m_c}, \quad a_2 = \frac{2nC_t}{m_c},$$

$$b_1 = \frac{\mu_{III}}{J_{lp}}\sum_{i=1}^{2n} l_i^2, \quad b_2 = \frac{C_t}{J_{lp}}\sum_{i=1}^{2n} l_i^2, \quad \dot{\iota} = 2.$$

where: C_t is the radial stiffness coefficient for tractor tires, μ_t is the viscous friction coefficient for tractor tires; J_{lp} represents the moment of inertia of the system in the longitudinal plane; l_i are the auxiliary coordinates associated with the road profile. The auxiliary coordinates refer to the path of the tire (J_i) that hits irregular surface. In this case, the center of mass will shift by the value Z.

Multiplying both sides of the expression (3) by $e^{-i\omega t}$ and integrating it from 0 to ∞ enables the use of Laplace transforms to transform the system of differential equations into a set of algebraic equations with respect to two transfer functions $W_Z(i\omega)$ and $W_\varphi(i\omega)$, as shown below:

$$W_Z(i\omega) = \frac{K_\omega^Z + iC_\omega^Z}{m_c[(a_2 - \omega^2) + ia_1\omega]} \qquad (4)$$

$$K_\omega^Z = C_{III}\sum_{i=1}^{2n} cos\tau_i\omega + \mu_{III}\omega\sum_{i=1}^{2n} sin\tau_i\omega,$$

$$C_\omega^Z = \mu_{III}\omega\sum_{i=1}^{2n} cos\tau_i\omega - C_{III}\sum_{i=1}^{2n} sin\tau_i\omega,$$

$$W_\varphi(i\omega) = \frac{K_\omega^\varphi + iC_\omega^\varphi}{J_{\Pi}[(b_2 - \omega^2) + ib_1\omega]} \qquad (5)$$

$$K_\omega^\varphi = C_{III}\sum_{i=1}^{2n} l_i cos\tau_i\omega + \mu_{III}\omega\sum_{i=1}^{2n} l_i sin\tau_i\omega,$$

$$C_\omega^\varphi = \mu_{III}\omega\sum_{i=1}^{2n} cos\tau_i\omega - C_{III}\sum_{i=1}^{2n} sin\tau_i\omega$$

where: ω is the vibration frequency and i is the imaginary unit.

The amplitude-frequency characteristics are taken as modules $|W_z(i\omega)|$ and $|W_\varphi(i\omega)|$, calculated with the profile parameters of the tractor system. The programming and all the calculations were conducted on Matlab for an 8×8 log truck and these skidding tractor models: TLK 4-01, TLK 6-01, TLK 6-02, and TLK 6-04. The general characteristics of the models are displayed in Table 1.

Systems management bases on operations research and optimization. According to the principles of operations research used to study various systems, objects and processes (Ahmad, 1989), each investigation consists of goal-oriented activities. An operation is a controlled event, which involves a series of actions intended to achieve specific goals. Any definite choice of the researcher is called a *decision*. Some decisions lead to better outcomes and are considered *optimal*. To find them, a quantitative criterion, also known as the *efficiency indicator* (W), is used (Ahmad, 1989). When choosing a solution, the preference goes to those that make the efficiency indicator (W) taken on the maximum, or the minimum, value. If the goal is to maximize the efficiency indicator, then it will be written as follows: $W=>$max, but if the intention is to minimize it, the expression would be $W=>$min.

The solution elements could be numbers, vectors, physical qualities (load mass, wheel arrangement), and so forth. The

Table 1
Wheeled forestry machine specifications.

Characteristic	TLK 4-01	TLK 6-01	TLK 6-02	TLK 6-04	8 × 8
Engine power, kW	132	147	147	147	316
Operating weight, kg	14,500	19,050	19,360	19,550	1900
Wheel arrangement	4 × 4	6 × 6	6 × 6	6 × 6	8 × 8
Range of operating speeds, km/h	8–30	0–32	0–30	0–32	0–50

arrangement of such elements and conditions (e.g., vehicle's carrying capacity and maximum speed) represents a set of *possible* solutions, designated as *X*, while *x* denotes a concrete solution. Note that *x* belongs to the set of possible solutions ($x \in X$).

The ultimate problem of minimizing soil compaction along the skid trail comes down to considering the road type, the skidding method, vehicle specifications, and driving speed. The fundamental difference between this study and previous publications is that it estimates the total compaction of the soil that occurs during the skidding cycle (this includes passes without load). In addition, the present study takes the threshold limits of soil density into account and considers load limits specified by the manufacturer. In operations research, such problems are known as inverse problems. In this study, the minimal soil compaction ρ_{min} acts as the efficiency indicator (*W*). For a specific skid trail, these could be the skid trail conditions (α) and tractor model (χ), which determines the skidding method. The formula would be:

$$W = W(\alpha, \chi) \tag{6}$$

For a set of conditions (α), it is necessary to find a solution $\chi = \chi^*$ that makes *W* take on the minimum value. This value can be denoted as follows:

$$W^* = min(W(\alpha, \chi)) \tag{7}$$

$$\chi \in x$$

Assume that W^* reached the minimum value $W(\alpha, \chi)$, taken over all solutions within the set of possible solutions.

By calculating soil density at the bottom of the rut, it is possible to evaluate the degree of soil compaction under the static load of the tractor (Grigorev et al., 2020c). The formula would be:

$$\rho_N = \rho_0 + \alpha_0 U \tag{8}$$

where: $\alpha_0 = \frac{\rho_0(1-v_0^2)}{E_0 H}$;

$U = \omega b q_{max v}(1 + \chi lgN)$; where: ρ_0 is soil density; *H* represents the depth of compaction; *b* is the width of the drive; v_0 denotes the coefficient of lateral expansion (Poisson's ratio); E_0 represents the deformation modulus of soil; χ is the coefficient of irreversible damage accumulation intensity under repeated loading; lg *N* is the decimal logarithm for the number of passes along one trail; ω is the coefficient depending on the size and shape of the supporting frame; $q_{max v}$ is the maximum load at speed *v*.

The Student's t test was used to assess the error in the estimated mean of the unevenness coefficient of soil compaction (State Agroindustrial Committee of the USSR, 1987). The unevenness coefficient ($\bar{\bar{\xi}}$) was obtained experimentally after the impact of the skidder. The mean value of the said coefficient was calculated using the following formula:

$$\bar{\bar{\xi}} = \frac{\sum_{i=1}^n \xi}{n} \tag{9}$$

where: ɳ is the number of examined sections; ξ is the unevenness coefficient of the soil compaction for a specific trail section:

$$\xi = \frac{L}{\pi D^*} \tag{10}$$

where: *L* is the length of the object's outer boundary, m; *D* is the diameter of a circle whose area is equal to the object area, m.

The error in the estimated mean was calculated using the formula below:

$$S_{\bar{\bar{\xi}}} = \sqrt{\frac{\sum_{i=1}^n (\xi_i - \bar{\bar{\xi}})^2}{n(n-1)}} \tag{11}$$

The relative error (δ) of the measurement was calculated by the formula:

$$\delta = \frac{S_{\bar{\bar{\xi}}}}{\bar{\bar{\xi}}} \cdot 100\% \tag{12}$$

The confidence interval of the coefficient ($\bar{\bar{\xi}}$) would be:

$$\bar{\bar{\xi}} \pm t_\beta S_{\bar{\bar{\xi}}} \tag{13}$$

where: t_β is the value of *t* in the two-sided *t*-test, where the level of significance is 0.05.

When δ is more than 5 percent, the procedure is repeated with a higher soil density.

Mathematical models were tested on the territory of the Namsky District of the Sakha Republic, the Russian Federation. The continental climate of the area has a negative impact on stands, especially on their root system, which develops exceptionally poorly. Soil dryness, in turn, leads to a slowdown in the growth and development of stands. The predominant species here are conifers (mainly pine, larch, and spruce), shrub willow, and dwarf birch. However, silver birch trees are also common. Plain areas are characterized by different types of soils: from clay to pebbles. Though, sandy, sandy loam, sod, sod-forest, meadow-chernozem soils can also be found. In the zone where the experimental research was held, sod-forest soil type and pine-larch plantations prevailed.

The growing stock limits of the felling area made it possible to estimate soil compaction after skidding cycles (passes with and without load). Each skidding tractor had a separate trail on the same types of soil, along which a number of passes were to be made. After the tractors passed the defined forest trails, soil density was measured. To determine the density of the soil along each trail, 60 cores were collected with a special device – soil penetrometer. Soil density measurements were taken after each skidding cycle.

3. Results and discussion

Figs. 1 and 2 show amplitude-frequency characteristic (AFC) curves computed for all skidders at different operating speeds using formulas (4) and (5) while taking into account the resistance forces of the unloaded tractor.

Wheeled skidders are generally constructed to have a power drive source at the front end of the frame and a functional accessory at the back end of the frame. The same design is used in 4 × 4 and 8 × 8 forwarders, but the vehicle dynamics are different. The difference between the two types of forestry machines is associated with mass, which is linked proportionally to the radial stiffness of tires. This aspect is seen from AFC graphs. As can be seen, all
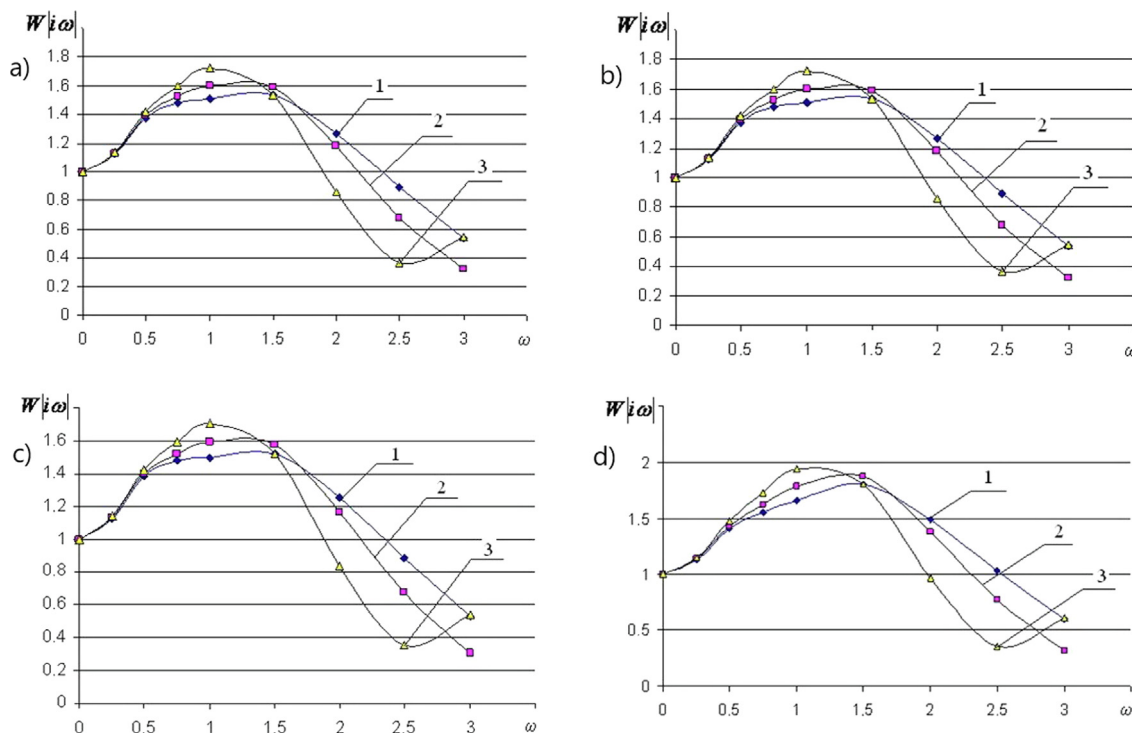
Fig. 1. The amplitude-frequency characteristics of unloaded vehicles: a) TLK 4-01; b) TLK 6-01; c) TLK 6-02; d) TLK 6-04; 1 – v = 3.0 m/sec; 2 – v = 2.5 m/sec; 3 – v = 2.0 m/sec.
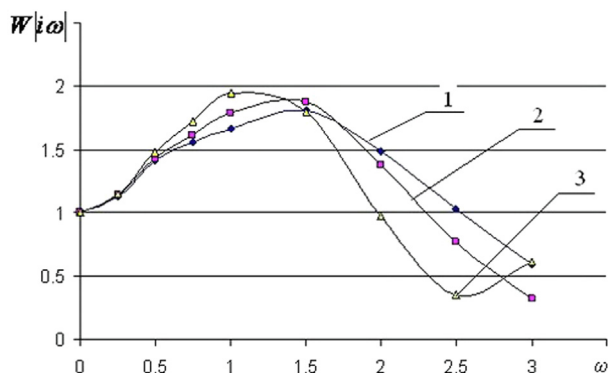

Fig. 2. The amplitude-frequency characteristics of the unloaded 8 × 8 truck: 1 – v = 3.0 m/sec; 2 – v = 2.5 m/sec; 3 – v = 2.0 m/sec.

of them display frequencies, which are close to the resonant frequency. Their values increase with increasing speed and are within the range of 1.0–1.5 m/sec.

The peak amplitudes of all AFC graphs are practically equal, which is not the case with vehicles operating at significantly higher speeds. This finding confirms the expediency of using AFC in the study of wheeled skidders.

When the dynamic system is loaded, the mass of its rear frame increases, and sometimes there is a relationship between the bundle of logs and the rear frame. This connection is depicted in AFC graphs.

Figs. 3 and 4 show amplitude-frequency characteristic curves computed for skidders operating at different speeds. The analysis of theoretical information revealed the overall soil compaction from different skidding machines and its dynamic component. The results are depicted in Table 2.

Data in Table 2 reveal a narrow range of soil density change under compaction stress caused by the weight of moving skidders.

For instance, the dynamic increment in compaction on the third skid trail ranges between 0.15 and 0.19 g/cm^3, while on the fifth one, it is within the range of 0.38 and 0.40 g/cm^3. TLK 4-01, on the other hand, caused greater damage in the form of overall soil compaction. The change in the density of soil caused by dynamic loading from TLK 4-01 ranges from 0.1 g/cm^3 along a forest road to 0.40 g/cm^3 when on the fifth skid trail. Note that the highest levels of compaction were obtained for skid trails five and six, associated with the highest values of mathematical expectation and the highest standard deviations of longitudinal unevenness. The ratio of dynamic to static soil densities gives a broad range of values. For example, it ranges between 45 and 165% for TLC 4-01 and between 32 and 90% for TLC 6-02. The likely reason is the dynamic properties of skidders and their interaction with the road profile.

Of greatest interest is the percentage of overall soil compaction from dynamic loading (Table 3). It varies between 23 and 50% (Fig. 5) for all skidding systems, including the promising 8 × 8 truck. It is even higher with 4 × 4 and 6 × 6 tractors in skid trails with significant unevenness, such as skid trails five and six, where it can reach 60 and even 66% (Fig. 6). The percentage of overall soil compaction on these skid trails reaches 98 to 99% under the dynamic load of the 8 × 8 truck. The dynamic skidding systems contribute the least (21–31%) to the overall soil compaction when they travel along a forest road with higher soil density and a more even surface profile.

There is a pattern of dependence between the level of overall soil compaction and the number of skidding cycles (Figs. 7 and 8). This pattern remains consistent with different skidders. When moving along the first four skid trails (the expected level of their surface unevenness is lower than that of skid trails five and six), 4 × 4 skidders can perform more than ten skidding cycles, and 6 × 6 skidders can only perform five to six of them. When moving along the other two skid trails, which have higher surface unevenness, these skidding systems can perform one or two cycles less before the maximum acceptable soil density (1.70 g/cm^3) is achieved. The 8 × 8 trucks compacts the soil more deeply, such
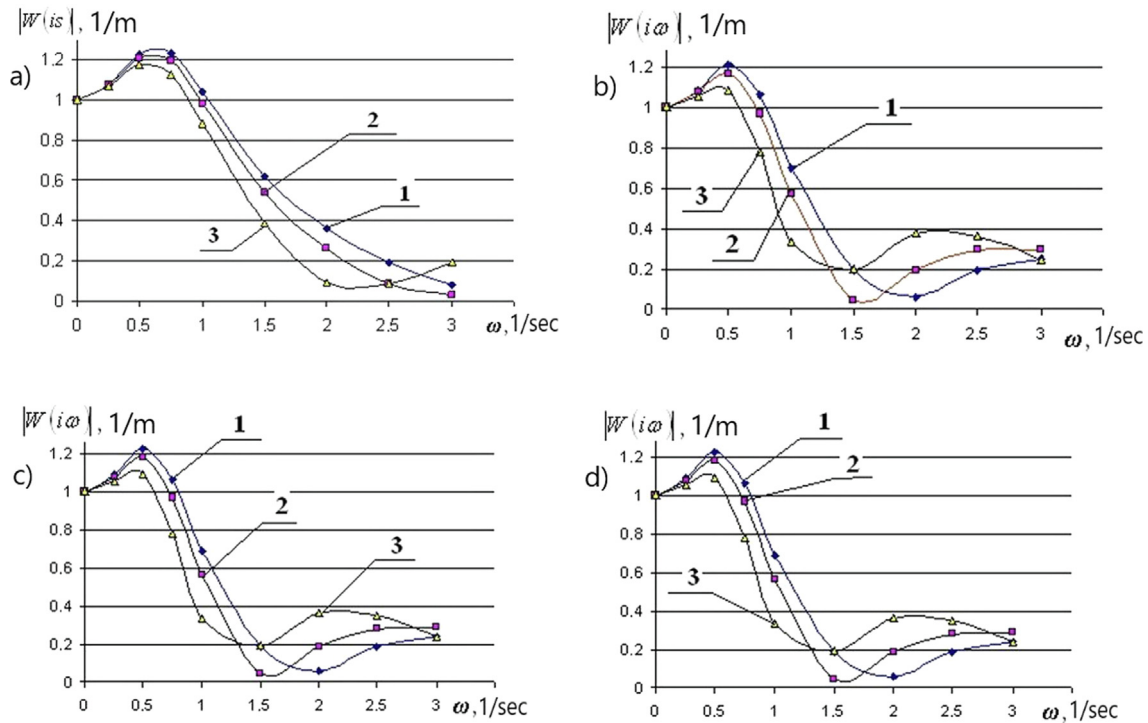
Fig. 3. The amplitude-frequency characteristics of skidders: a) TLK 4–01: 1 – υ = 2.22 m/sec; 2 – υ = 1.9 m/sec; 3 – υ = 1.4 m/sec; b) TLK 6-01; c) TLK 6-02; d) TLK 6-04; 1 – υ = 1.0 m/sec; 2 – υ = 0.9 m/sec; 3 – υ = 0.8 m/sec.
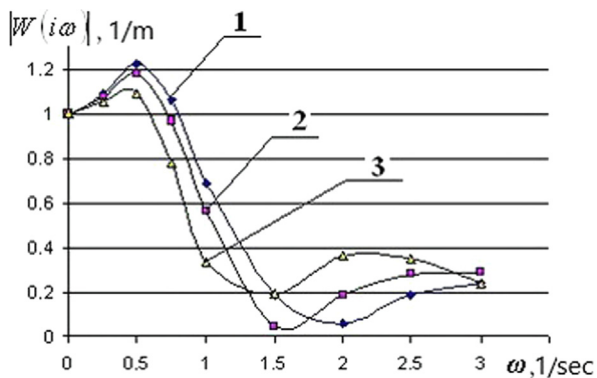
Fig. 4. The amplitude-frequency characteristics of the loaded 8 × 8 truck: 1 – υ = 3.0 m/sec; 2 – υ = 2.5 m/sec; 3 – υ = 2.0 m/sec.

that it reaches the compaction threshold practically after the first skidding cycle. Therefore, 8 × 8 skidding systems can only be used during the cold season when the soil is frozen.

Figs. 9 and 10 show theoretical and experimental dependences of soil density and the number of skidding cycles for different skid trails versus a forest road. The difference between the experimental and theoretical values of soil density does not exceed 12%. Given the complexity of mathematical models for the tractor/bundle-of-logs/soil system, such a narrow range of soil density values suggests the high reliability of the results. For verification, mathematical expectations were compared with experimental data. No significant differences were found.

Table 4 shows the values of the compaction unevenness coefficient with the confidence probability β = 0.95. The mean value ($\bar{\xi}$) of the coefficient is 0.02 g/cm³. The error of the mean ($S_{\bar{\xi}}$) is 0.00012 g/cm³, and the relative error (δ) is 6%. Given the complexity of the study object, these figures can be considered acceptable. With the t-value of 2.13 (Grigorev et al., 2020a), the mean value ($\bar{\xi}$)

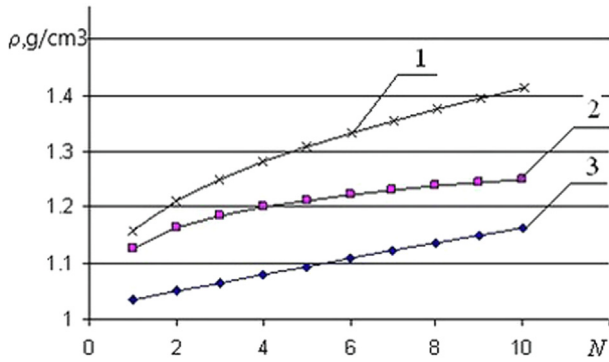**Table 2**
Overall soil compaction.

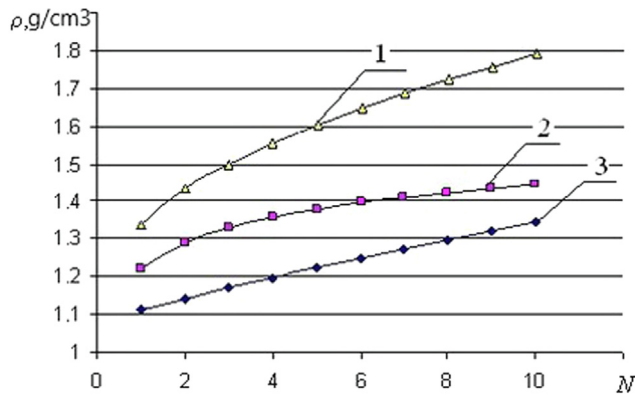| Skid trail	Vehicle									
	TLK 4-01		sTLK 6-01		TLK 6-02		TLK 6-04		8 × 8 truck	
	ρ_d	ρ_d/ρ_{stat}	ρ_d	ρ_d/ρ_{stat}	ρ_d	ρ_d/ρ_{stat}	ρ_d	ρ_d/ρ_{stat}	ρ_d	ρ_d/ρ_{stat}
1	0.15	64	0.14	35	0.14	32	0.15	34	0.18	30
2	0.23	90	0.20	50	0.23	53	0.23	51	0.23	36
3	0.15	62	0.15	37	0.15	35	0.18	42	0.19	30
4	0.25	100	0.23	57	0.24	56	0.24	53	0.28	46
5	0.40	165	0.38	95	0.38	90	0.38	85	0.40	65
6	0.36	148	0.33	80	0.32	55	0.32	78	0.38	61
Forest road	0.10	45	0.11	27	0.14	33	0.14	32	0.15	25

Note: ρ_d denotes soil density under the dynamic load, g/cm³; ρ_d/ρ_{stat} is the ratio dynamic to static soil densities, %.

Table 3
Overall soil compaction under dynamic loading.

Skid trail	Vehicle									
	TLK 4-01		TLK 6-01		TLK 6-02		TLK 6-04		8 × 8 truck	
	ρ_Σ, g/cm³	ρ_d/ρ_Σ, %	ρ_Σ, g/cm³	ρ_d/ρ_Σ, %	ρ_Σ, g/cm³	ρ_d/ρ_Σ, %	ρ_Σ, g/cm³	ρ_d/ρ_Σ, %	ρ_Σ, g/cm³	ρ_d/ρ_Σ, %
1	0.38	39	0.54	26	0.58	24	0.59	25	0.78	23
2	0.48	48	0.60	33	0.66	35	0.68	34	0.86	27
3	0.39	38	0.56	27	0.58	26	0.60	30	0.82	28
4	0.49	50	0.63	36	0.67	30	0.69	35	0.89	31
5	0.60	60	0.76	50	0.8	47	0.82	46	1.01	99
6	0.60	60	0.74	45	0.9	35	0.73	44	1.00	98
Forest road	0.32	31	0.52	21	0.56	25	0.58	24	0.60	25

Fig. 5. The relationship between soil density on the third skid trail and the number of skidding cycles with TLK 4-01: 1 – total compaction of soil; 2 – compaction from static loading; 3 – compaction from dynamic loading.
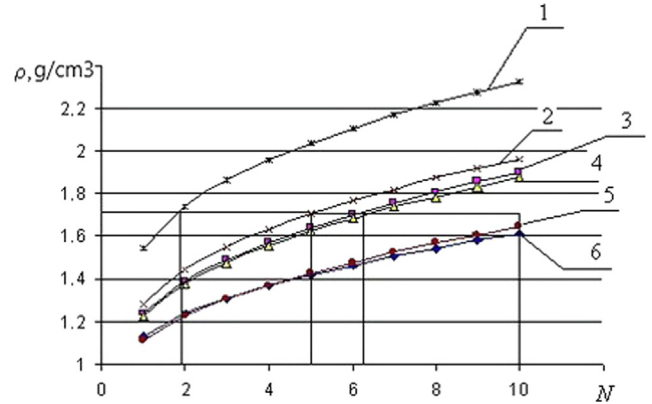

Fig. 7. The relationship between soil density on the third skid trail and the number of skidding cycles with the following vehicles: 1 – 8 × 8 truck; 2 – TLK 6-04; 3 – TLK 6-02; 4 – TLK 6-01; 5 – 4 × 4 tractor; 6 – TLK 4-01.

Fig. 6. The relationship between soil density on the third skid trail and the number of skidding cycles with TLK 6-04: 1 – total compaction of soil; 2 – compaction from static loading; 3 – compaction from dynamic loading.

Fig. 8. The relationship between soil density on the sixth skid trail and the number of skidding cycles with the following vehicles: 1 – 8 × 8 truck; 2 – TLK 6-04; 3 – TLK 6-02; 4 – TLK 6-01; 5 – 4 × 4 tractor; 6 – TLK 4-01.

of the coefficient would be 0.02 ± 0.00025 g/cm³. The experimental data on soil density thus show that a skid trail has a slightly uneven surface profile.
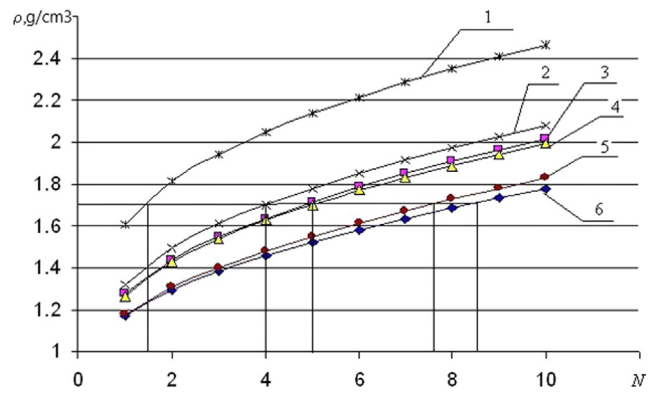
A similar but simpler technique was proposed in the work of Wenzel (1962), which uses the confidence probability (β). If the random variable distribution law is known, it is possible to find the precise confidence interval (J_β) for a specific probability (such as β = 0.90–0.95). When the random variable x has normal distribution, which the soil density follows, it obeys the Student's distribution law, as shown below:

$$T = \sqrt{n}\frac{\tilde{m} - m}{\sqrt{D}}, \tag{14}$$

where: n is the number of trials.

$$\tilde{m} = \frac{\sum_{i=1}^{n} x_i}{n}; D = \frac{\sum_{i=1}^{n}\left(x_i - \tilde{m}\right)^2}{n-1}. \tag{15}$$

To determine the confidence interval (J_β), it is necessary to find such a value of t_β that

$$P(|T| < t_\beta) = \beta. \tag{16}$$

At least 20 trials were conducted to determine the density of the soil along the skid trail. Some authors provided tables of t_β values that depend on the confidence probability β and the degree of freedom n-1 (Mitkov and Kardashevsky, 1978). Once the value of t_β is known, assume that the error of the confidence interval is
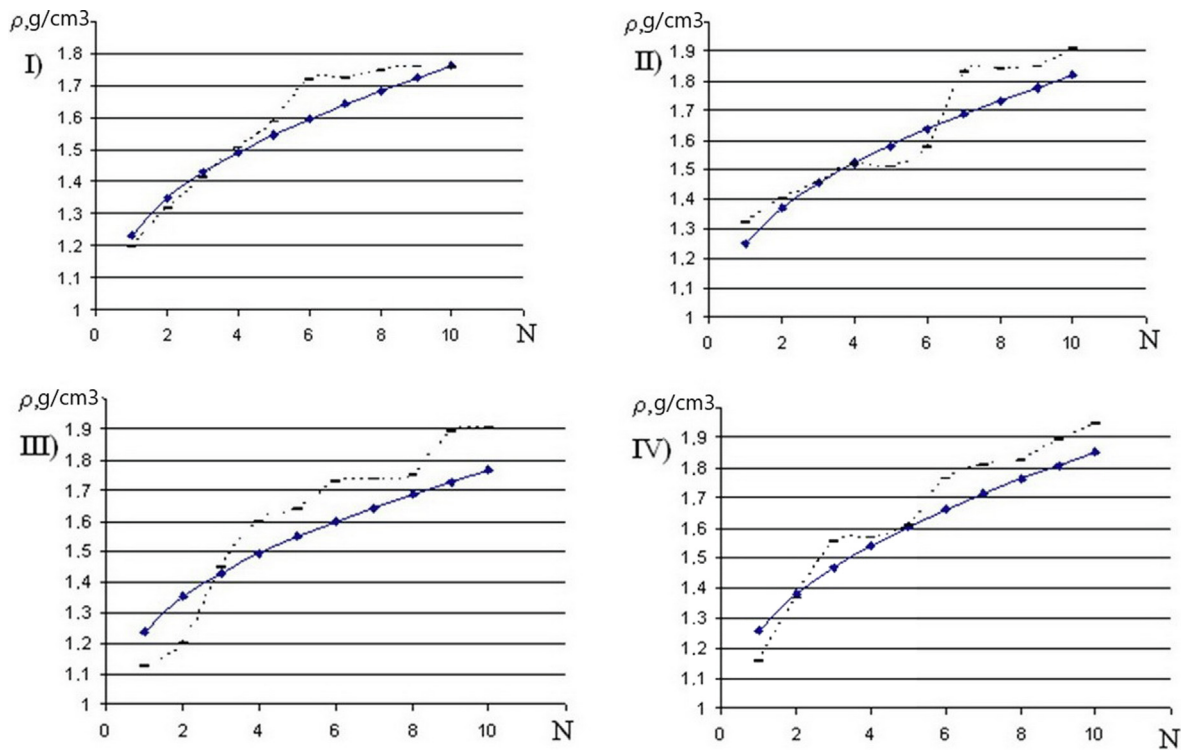
Fig. 9. Theoretical (solid line) and experimental (dotted line) relationship between soil density (ρ) and the number of skidding cycles (N): I – first skid trail; II – second skid trail; III – third skid trail; IV – fourth skid trail.
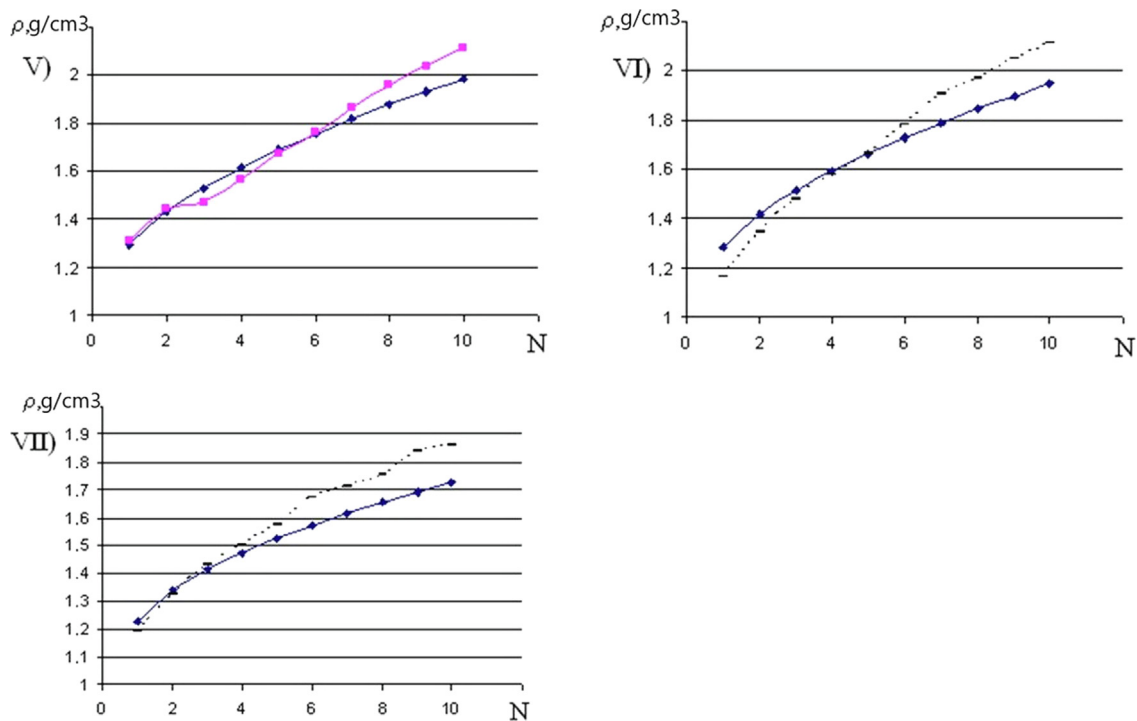

Fig. 10. Theoretical (solid line) and experimental (dotted line) relationship between soil density (ρ) and the number of skidding cycles (N): V – fifth skid trail; VI – sixth skid trail; VII – forest road.

$$\varepsilon_\beta = t_\beta \sqrt{\frac{D}{n}}. \tag{17}$$

In doing so, it is possible to determine half the width of the confidence interval and the confidence interval itself. The formula would be:

$$J_p = (\tilde{m} - t_\beta \sqrt{\frac{D}{T}}\tilde{m} + t_\beta \sqrt{\frac{D}{T}}). \tag{18}$$

For 20 trials, $\beta = 0.90$ and $t_\beta = 1.725$; hence, $D = 0.14$ g/cm³ and $\varepsilon_\beta = 0.11$ with $\tilde{m} = 1.6$ g/cm³. The confidence interval will be $J_\beta = 1.6 \pm 0.11$ g/cm³. Insignificant differences between the the-

Table 4
Analysis of the soil compaction unevenness.

Number of trial	ρ, g/cm^3	ξ, g/cm^3	$\xi - \bar{\xi}$, g/cm^3	$(\xi - \bar{\xi})^2$
1	1.57	0.03	0.01	0.0001
2	1.60	0.00	–	–
3	1.58	0.02	0.00	–
4	1.63	0.03	0.01	0.0001
5	1.56	0.04	0.02	0.0004
6	1.60	0.00	0.00	–
7	1.57	0.03	0.01	0.0001
8	1.62	0.00	–	–
9	1.60	0.00	–	–
10	1.63	0.03	0.01	0.0001
11	1.57	0.03	0.01	0.0001
12	1.60	0.00	–	–
13	1.64	0.04	0.02	0.0004
14	1.63	0.03	0.01	0.0001
15	1.60	0.00	–	–

oretical and experimental values of the overall soil compaction, along with the admissible values of the unevenness coefficient of soil compaction and the confidence interval, indicate the adequacy of the mathematical models (Grigorev et al., 2020a, 2020b, 2021).

4. Conclusions

The paper reports the results of a study of soil compaction under dynamic loading from different types of wheeled forest machines. The amplitude-frequency characteristics of the tractor/bundle-of-logs/soil system show no substantial differences in amplitude response between the studied tractors. The analysis of soil compaction from dynamic loading revealed that 23 to 50% of compaction occurs in the first four skid trails. Higher compaction occurs in skid trails with significant unevenness. However, the 8×8 truck (98–99%) compacted the soil more than 4×4 and 6×6 skidders (60–66%). The least compaction (21–31%) from dynamic loading occurs on the forest road. The difference between the experimental and theoretical values of soil density does not exceed 12%, which falls within the acceptable range. The mathematical models are in good agreement with the experimental data and can be used to calculate the operating modes of wheeled forestry equipment.

Declaration of Competing Interest

The authors declare that they have no known competing financial interests or personal relationships that could have appeared to influence the work reported in this paper.

Data Availability

Data will be available on request.

References

Abukari, A., Christian, D., Ochire-Boadu, K., 2021. Bulk density and porosity of soils influenced by skidding operations in the Nkrankwanta Off-Forest Reserve of Ghana. Adv. For. Sci. 8 (2), 1409–1415. https://doi.org/10.34062/afs.v8i2.9530.

Ahmad, S.H., 1989. Simple enumeration of minimal tiesets of undirected graph. Microelectronics Reliab. 29 (4), 509–510. https://doi.org/10.1016/0026-2714(89)90335-1.

Allman, M., Merganič, J., Merganičová, K., 2020. Machinery-induced damage to soil and remaining forest stands—Case study from Slovakia. Forests 11 (12), 1289. https://doi.org/10.3390/f11121289.

Aust, W.M., Bolding, M.C., Barrett, S.M., 2020. Silviculture in forested wetlands: summary of current forest operations, potential effects, and long-term experiments. Wetlands 40 (1), 21–36. https://doi.org/10.1007/s13157-019-01191-6.

Bigelow, S.W., Jansen, N.A., Jack, S.B., Staudhammer, C.L., 2018. Influence of selection method on skidder-trail soil compaction in longleaf pine forest. For. Sci. 64 (6), 641–652. https://doi.org/10.1093/forsci/fxy023.

Cambi, M., Hoshika, Y., Mariotti, B., Paoletti, E., Picchio, R., Venanzi, R., Marchi, E., 2017. Compaction by a forest machine affects soil quality and Quercus robur L. seedling performance in an experimental field. For. Ecolo. Manag. 384, 406–414. https://doi.org/10.1016/j.foreco.2016.10.045.

Cambi, M., Mariotti, B., Fabiano, F., Maltoni, A., Tani, A., Foderi, C., Laschi, A., Marchi, E., 2018. Early response of Quercus robur seedlings to soil compaction following germination. Land Degrad. Dev. 29 (4), 916–925. https://doi.org/10.1002/ldr.2912.

Grigorev, I., 2005. Characteristics of the micro-profiles of skid trails determining the dynamic compaction of soils. In: Panfilov, A.Y. (Ed.), Collection of scientific papers "Pressing challenges of the forestry complex", vol. 10, Bryansk, pp. 10–13.

Grigorev, I., Kunickaya, O., Burgonutdinov, A., Burmistrova, O., Druzyanova, V., Dolmatov, N., Voronova, A., Kotov, A., 2021. Modeling the effect of skidded timber bunches on forest soil compaction. J. Def. Model. Simul. https://doi.org/10.1177/1548512920978700 (in press).

Grigorev, I., Kunickaya, O., Burgonutdinov, A., Burmistrova, O., Druzyanova, V., Dolmatov, N., Voronova, A., Kotov, A., 2020a. Assessment the effect of skidding techniques on the ecological efficiency of the skidding tractor. Diagnostyka 21 (3), 67–75. https://doi.org/10.29354/diag/125311.

Grigorev, I., Kunickaya, O., Burgonutdinov, A., Ivanov, V., Shuvalova, S., Shvetsova, V., Stepanishcheva, M., Tikhonov, E., 2020b. Theoretical studies of dynamic soil compaction by wheeled forestry machines. Diagnostyka 21 (4), 3–13. https://doi.org/10.29354/diag/127650.

Grigorev, I., Kunickaya, O., Prosuzhih, A., Kruchinin, I., Shakirzyanov, D., Shvetsova, V., Markov, O., Egipko, S., 2020c. Efficiency improvement of forest machinery exploitation. Diagnostyka 21 (2), 95–109. https://doi.org/10.29354/diag/122797.

Ivanov, V.A., Grigorev, I.V., Gasparyan, G.D., Manukovsky, A.Y., Zhuk, A.Y., Kunitskaya, O.A., Grigoreva, O.I., 2018. Environment-friendly logging in the context of water logged soil and knob-and-ridge terrain. J. Mech. Eng. Res. Dev. 41 (2), 22–27. https://doi.org/10.26480/jmerd.02.2018.22.27.

Kremers, J., Boosten, M., 2018. Soil compaction and deformation in forest exploitation. Am. J. Alternative Agric. 7 (1–2), 25–31.

Lynch, T.D., 2020. Organization Theory and Management. Routledge.

Manukovsky, A.Y., Grigorev, I.V., Ivanov, V.A., Gasparyan, G.D., Lapshina, M.L., Makarova, Y.A., Chetverikova, I.V., Yakovlev, K.A., Afonichev, D.N., Kunitskaya, O.A., 2018. Increasing the logging road efficiency by reducing the intensity of rutting: mathematical modeling. J. Mech. Eng. Res. Dev. 41 (2), 35–41. https://doi.org/10.26480/jmerd.02.2018.36.42.

Mitkov, A.P., Kardashevsky, S.V., 1978. Statistical methods in agricultural engineering. Mashinostroyeniye, Moscow.

Mohieddinne, H., Brasseur, B., Spicher, F., Gallet-Moron, E., Buridant, J., Kobaissi, A., Horen, H., 2019. Physical recovery of forest soil after compaction by heavy machines, revealed by penetration resistance over multiple decades. For. Ecol. Manag. 449, 117472. https://doi.org/10.1016/j.foreco.2019.117472.

Naghdi, R., Solgi, A., Zenner, E.K., Najafi, A., Salehi, A., Nikooy, M., 2017. Compaction of forest soils with heavy logging machinery. Silva Balc. 18 (1), 25–39.

Parkhurst, B.M., Aust, W.M., Bolding, M.C., Barrett, S.M., Carter, E.A., 2018. Soil response to skidder trafficking and slash application. Int. J. For. Eng. 29 (1), 31–40. https://doi.org/10.1080/14942119.2018.1413844.

Rudov, S.E., Voronova, A.M., Chemshikova, J.M., Teterevleva, E.V., Kruchinin, I.N., Dondokov, Y.Z., Khaldeeva, M.N., Burtseva, I.A., Danilov, V.V., Grigorev, I.V., 2019. Theoretical approaches to logging trail network planning: increasing efficiency of forest machines and reducing their negative impact on soil and terrain. Asian J. Water Environ. Pollut. 16 (4), 61–75. https://doi.org/10.3233/AJW190049.

Sealey, L.L., Van Rees, K.C., 2019. Influence of skidder traffic on soil bulk density, aspen regeneration, and vegetation indices following winter harvesting in the Duck Mountain Provincial Park. SK. For. Ecol. Manag. 437, 59–69. https://doi.org/10.1016/j.foreco.2019.01.017.

Solgi, A., Naghdi, R., Marchi, E., Laschi, A., Keivan Behjou, F., Hemmati, V., Masumian, A., 2019a. Impact assessment of skidding extraction: Effects on physical and chemical properties of forest soils and on maple seedling growing along the skid trail. Forests 10 (2), 134. https://doi.org/10.3390/f10020134.

Solgi, A., Naghdi, R., Zenner, E.K., Tsioras, P.A., Hemmati, V., 2019b. Effects of ground-based skidding on soil physical properties in skid trail switchbacks. Croat. J. For. Eng. 40 (2), 341–350. https://doi.org/10.5552/crojfe.2019.535.

Spinelli, R., Magagnotti, N., Cavallo, E., Capello, G., Biddoccu, M., 2019. Reducing soil compaction after thinning work in agroforestry plantations. Agrofor. Syst. 93 (5), 1765–1779. https://doi.org/10.1007/s10457-018-0279-6.

State Agroindustrial Committee of the USSR, 1987. GOST 26953-86: Agricultural mobile machinery. Methods for determining force produced by propelling agents on soil. Date of adoption: 1987-01-01.

Tavankar, F., Picchio, R., Nikooy, M., Jourgholami, M., Latterini, F., Venanzi, R., 2021a. Effect of soil moisture on soil compaction during skidding operations in poplar plantation. Int. J. For. Eng. 32 (2), 128–139. https://doi.org/10.1080/14942119.2021.1878802.

Tavankar, F., Picchio, R., Nikooy, M., Jourgholami, M., Naghdi, R., Latterini, F., Venanzi, R., 2021b. Soil natural recovery process and Fagus orientalis lipsky seedling growth after timber extraction by wheeled skidder. Land 10 (2), 113. https://doi.org/10.3390/land10020113.

Ugawa, S., Inagaki, Y., Karibu, F., Tateno, R., 2020. Effects of soil compaction by a forestry machine and slash dispersal on soil N mineralization in Cryptomeria japonica plantations under high precipitation. New For. 51 (5), 887–907. https://doi.org/10.1007/s11056-019-09768-z.

Vantellingen, J., Thomas, S.C., 2021. Skid trail effects on soil methane and carbon dioxide flux in a selection-managed Northern Hardwood forest. Ecosystems 24, 1402–1421. https://doi.org/10.1007/s10021-020-00591-8.

Wenzel, E.S., 1962. Probability theory. Fiziko-Matematicheskaya Literature, Moscow.

Yazarlou, H., Parsakhoo, A., Habashi, H., Soltauninejad, S.A., 2017. Effect of the skid trail cross section and horizontal alignment on forest soil physical properties. For. Sci. 63 (4), 161–166. https://doi.org/10.17221/108/2016-JFS.